Inorganic Chemistry
Article

Inorg. Chem. **2010**, *49*, 11205–11215 **11205**
DOI: 10.1021/ic101830e

Solid-State ^{15}N CPMAS NMR and Computational Analysis of Ligand Hapticity in Rhodium(η-diene) Poly(pyrazolyl)borate Complexes

Riccardo Pettinari,[†] Claudio Pettinari,*[,†] Fabio Marchetti,[‡] Roberto Gobetto,*[,§] Carlo Nervi,[§] Michele R. Chierotti,[§] Eric J. Chan,[∥] Brian W. Skelton,[∥] and Allan H. White[∥]

[†]*School of Pharmacy, and* [‡]*School of Science & Technology, University of Camerino, Via S. Agostino 1, 62032 Camerino, Italy,* [§]*Dipartimento di Chimica IFM, University of Torino, Via P. Giuria 7, 10125 Torino, Italy, and* [∥]*Chemistry M313, SBBCS, The University of Western Australia, Crawley, Western Australia, 6009, Australia*

Received September 6, 2010

Novel [Rh(η-diene)Tp^x] complexes of sterically encumbered Tp^x ligands (Tp^x = Tp^{4Bo}, diene = cod, **1**; nbd, **2**; Tp^x = Tp^{4Bo,5Me}, diene = cod, **3**; nbd, **4**; Tp^x = Tp^{a,3Me}, diene = cod, **5**; nbd, **6**; Tp^x = Tp^{a*,3Me}, diene = cod, **7**; nbd, **8**) have been prepared by treatment of [Rh(η-diene)(μ-Cl)]$_2$ with TlTp^x (Tp^x in general, in detail: Tp^{4Bo} = hydrotris(indazol-1-yl)borate, Tp^{4Bo,5Me} = hydrotris(5-methyl-indazol-1-yl)borate, Tp^{a,3Me} = hydrotris(3-methyl-2*H*-benz[*g*]-4,5-dihydroindazol-2-y1)borate, Tp^{a*,3Me} = hydrotris(3-methyl-2*H*-benz[*g*]indazol-2-yl)borate), and characterized by analytical and spectral data (IR, ^{1}H, ^{11}B, and ^{13}C NMR solution). The structures adopted by [Rh(nbd)Tp^{4Bo}] **2**, [Rh(cod)Tp^{4Bo,5Me}] **3**, [Rh(nbd)Tp^{a,3Me}] **6**, [Rh(nbd)Tp^{a*,3Me}] **8**, and [Rh(nbd)Tp^{a*,3Me*}] **8*** (incorporating a borotropomeric ligand), have been investigated. Low steric hindrance between the ligands in **2** and **3** permits κ^3 coordination of the pyrazolylborate while the high steric encumbrance present in **6**, **8**, and **8*** results in κ^2 ligands. The coordination modes of the ligands to the metal have also been established by ^{15}N CPMAS studies of selected ligands and their corresponding Rh complexes. These spectroscopic data are in agreement with the ^{15}N chemical shifts obtained by using quantum-chemical methods to assist reliable assignments of the experimental values, affording new insights into the extraction of structural information concerning the hapticity (κ^2 or κ^3) of the poly(pyrazolyl)borate ligands to the Rh metal.

Introduction

Hydrotris(1-pyrazolyl)borates (Tp^x) have been recognized as versatile ligands in the fields of both coordination and organometallic chemistry.[1] During the past four decades it has been shown that the range of applicability of these ligands can be extended even further in these two areas, and several pyrazolylborates or scorpionate complexes are now available which show promise in materials science,[2] homogeneous catalysis,[3] and bioinorganic chemistry.[4] Tp^x ligands bind predominantly in a facial κ^3-*N*,*N*′,*N*″-tripodal fashion, and examples of κ^2-Tp^{x}ML$_n$ complexes are rare except among 16-electron, square-planar species.[1,2,5] For complexes like [Rh(cod)Tp^x] (cod = cyclooctadiene), "square planar" (spl) coordination geometry has been always found,[6−11] where the Tp^x behave as κ^2-bidentate ligands, the only exception being represented

*To whom correspondence should be addressed. E-mail: claudio.pettinari@unicam.it.

(1) (a) Trofimenko, S. *Scorpionates: The Coordination Chemistry of Polypyrazolylborates Ligands*; Imperial College Press: London, 1999. (b) Pettinari, C.; *Scorpionates II: Chelating Borate Ligands*; Imperial College Press: London, 2008.

(2) (a) Guo, S. L.; Peters, F.; Fabrizi de Biani, F.; Bats, J. W.; Herdtweck, E.; Zanello, P.; Wagner, M. *Inorg. Chem.* **2001**, *40*, 4928–4936. (b) Haghiri Ilkhechi, A.; Mercero, J. M.; Silanes, I.; Bolte, M.; Scheibitz, M.; Lerner, H.-W.; Ugalde, J. M.; Wagner, M. *J. Am. Chem. Soc.* **2005**, *127*, 10656–10666.

(3) (a) Bieller, S.; Zhang, F.; Bolte, M.; Bats, J. W.; Lerner, H.-W.; Wagner, M. *Organometallics* **2004**, *23*, 2107–2113. (b) Bieller, S.; Bolte, M.; Lerner, H.-W.; Wagner, M. *Inorg. Chem.* **2005**, *44*, 9489–9496.

(4) (a) Ruth, K.; Tüllmann, S.; Vitze, H.; Bolte, M.; Lerner, H.-W.; Holthausen, M. C.; Wagner, M. *Chem.—Eur. J.* **2008**, *14*, 6754–6770. (b) Tesmer, M.; Shu, M.; Vahrenkamp, H. *Inorg. Chem.* **2001**, *40*, 4022–4029. (c) Parkin, G. *Adv. Inorg. Chem.* **1995**, *42*, 291–393. (d) Alsafasser, R.; Trofimenko, S.; Looney, A.; Parkin, G.; Vahrenkamp, H. *Inorg. Chem.* **1991**, *30*, 4098–4100. (e) Bergquist, C.; Storrie, H.; Koutcher, L.; Bridgewater, B. M.; Friesner, R. A.; Parkin, G. *J. Am. Chem. Soc.* **2000**, *122*, 12651–12658.

(5) Trofimenko, S. *Chem. Rev.* **1993**, *93*, 943–980.

(6) Akita, M.; Ohta, K.; Takahashi, Y.; Hikichi, S.; Moro-oka, Y. *Organometallics* **1997**, *16*, 4121–4128.

(7) (a) Cocivera, M.; Desmond, T. J.; Ferguson, G.; Kaitner, B.; Lalor, F. J.; O'Sullivan, D. *Organometallics* **1982**, *1*, 1125–1132. (b) Cocivera, M.; Ferguson, G.; Kaitner, B.; Lalor, F. J.; O'Sullivan, D.; Parvez, M.; Ruhl, B. *Organometallics* **1982**, *1*, 1132–1139. (c) Cocivera, M.; Ferguson, G.; Lalor, F. J.; Szczecinski, P. *Organometallics* **1982**, *1*, 1139–1142.

(8) Santa Maria, M. D.; Claramunt, R. M.; Campo, J. A.; Cano, M.; Criado, R.; Heras, J. V.; Ovejero, P.; Pinilla, E.; Torres, M. R. *J. Organomet. Chem.* **2000**, *605*, 117–126.

(9) (a) Rheingold, A. L.; Haggerty, B. S.; Yap, G. P. A.; Trofimenko, S. *Inorg. Chem.* **1997**, *36*, 5097–5103. (b) Rheingold, A. L.; Liable-Sands, L. M.; Trofimenko, S. *Inorg. Chem.* **2000**, *39*, 1333–1335. (c) Bortolin, M.; Bucher, U. E.; Rüegger, H.; Venanzi, L. M.; Albinati, A.; Lianza, F.; Trofimenko, S. *Organometallics* **1992**, *11*, 2514–2521. (d) Rheingold, A. L.; Incarvito, C. D.; Trofimenko, S. *Inorg. Chem.* **2000**, *39*, 5569–5571.

(10) Ruman, T.; Ciunik, Z.; Trzeciak, A. M.; Wołowiec, S.; Ziółkowski, J. J. *Organometallics* **2003**, *22*, 1072–1080.

(11) Ruman, T.; Ciunik, Z.; Wołowiec, S. *Polyhedron* **2004**, *23*, 219–223.

Published on Web 10/27/2010

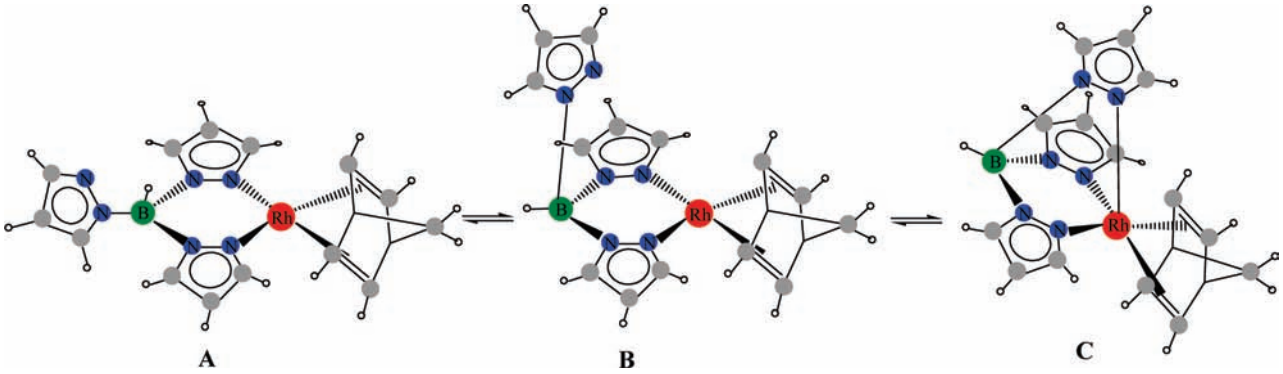

Figure 1. Fast equilibrium existing in solution between four- (**A** and **B**) and five-coordinate forms (**C**) of [Rh(diene)Tp^x] complexes.

by the recently reported [Rh(cod)Tp] which contains a κ^3-tridentate ligand,[12] as previously postulated by Venanzi and co-workers on the basis of solution ^{103}Rh NMR data.[13] 18-Electron trigonal-bipyramidal species are prevalent in [Rh(nbd)Tp^x] (nbd = norbornadiene) type complexes,[13,14] but examples have also been reported with spl geometry.[15]

The behavior in solution of these complexes has been investigated by NMR techniques, demonstrating that these species can interconvert among the three isomeric forms **A**, **B**, and **C** represented in Figure 1.[12,13] The **B**-**C** conversion is fast on the ^{1}H NMR time scale, resulting in averaging of all pyrazolyl resonances, whereas the **A**-**B** interconversion is relatively slower. In the solid state the isomer **A** has been established by X-ray crystallography only for [Rh(cod)Tp^{Ph}],[15] whereas isomer **C** has been found mainly in nbd derivatives. However, in solution all of the above compounds exist as mixtures of **A** and **C** species at concentrations which depend on temperature and solvent.

Analogous [Ir(diene)Tp^x] complexes have been investigated by Venanzi and co-workers,[16] focusing on their hydrolytic stabilities, and on the 1,2-borotropic rearrangement of pyrazolyl rings.

A further reason for extending the investigation of [M(diene)Tp^x] structural and spectroscopic properties, the study of their solution behavior, and the factors governing the ligand hapticity, arises from the discovery that [Rh(η^4-1,3-cod)Tp*], prepared by photoinduced intramolecular rearrangement of [Rh(η^4-1,5-cod)Tp*], is a versatile entry point into relevant organometallic reactivity.[17,18] [Rh(cod)Tp^x] complexes have been demonstrated to be efficient catalysts of the stereoregular polymerization of phenylacetylene,[19] also when used in ionic liquids.[20] More recently, [Rh(cod)Tp*] has been indicated as an active catalyst in alkyne hydrophosphinylation.[21] Monomeric tetrakis(pyrazolyl)borate complexes [M(diene)(κ^2-pzTp)] (M = Rh or Ir, diene = cod or nbd) have been employed to give homo- [(diene)M(μ-pzTp)M(diene)] and hetero-dinuclear [(diene)M(μ-pzTp)M′Cl$_2$] complexes.[22]

In extension of our previous work on rhodium derivatives containing scorpionate ligands,[23] we have undertaken a systematic study of the reactions between the [Rh(η-diene)(μ-Cl)]$_2$ dimers (diene = cod or nbd) and the variously substituted, poorly investigated until now, tris(pyrazolyl)borate ligands (Tp^{4Bo} = hydrotris(indazol-1-yl)borate, Tp^{4Bo,5Me} = hydrotris-(5-methyl-indazol-1-yl)borate, Tp^{a,3Me} = hydrotris(3-methyl-2*H*-benz[*g*]-4,5-dihydroindazol-2-yl)borate, Tp^{a*,3Me} = hydrotris(3-methyl-2*H*-benz[*g*]indazol-2-yl)borate), to ascertain, by combining ^{15}N CPMAS spectroscopy and computational data, how structural changes depend on the steric properties of the Tp^x. In the ligands Tp^{4Bo} and Tp^{4Bo,5Me} (Chart 1) the boron atoms are bonded exclusively to the more hindered,[9,24−26] but electronically richer, nitrogen atoms, representing a special class of homoscorpionate ligands which provide a protective pocket around the boron atoms, but are sterically less encumbered at the coordinating site, very similar to the parent Tp. At the same time the homoscorpionate ligands Tp^{a,3Me} and Tp^{a*,3Me} have the boron bonded exclusively to the less hindered nitrogen (Chart 1).[27] For comparison purposes also the analogous Tp and Tp* rhodium complexes ([Rh-(cod)Tp] (**9**), [Rh(nbd)Tp] (**10**), [Rh(cod)Tp*] (**11**) [Rh(nbd)-Tp*] (**12**), have been here reported and studied with the same techniques.

Experimental Section

Materials and Methods. The reagent, [Rh(η-diene)(μ-Cl)]$_2$, was purchased from Alfa (Karlsruhe) and used as received. All

(12) Adams, C. J.; Anderson, K. M.; Charmant, J. P. H.; Connelly, N. G.; Field, B. A.; Hallett, A. J.; Horne, M. *Dalton Trans.* **2008**, 2680–2692.
(13) Bucher, U. E.; Currao, A.; Nesper, R.; Rüegger, H.; Venanzi, L. M.; Younger, E. *Inorg. Chem.* **1995**, *34*, 66–74.
(14) Bucher, U. E.; Fässler, T. F.; Hunziker, M.; Nesper, R.; Rüegger, H.; Venanzi, L. M. *Gazz. Chim. Ital.* **1995**, *125*, 181–188.
(15) Sanz, D.; Santa Maria, M. D.; Claramunt, R. M.; Cano, M.; Heras, J. V.; Campo, J. A.; Ruîz, F. A.; Pinilla, E.; Monge, A. *J. Organomet. Chem.* **1996**, *526*, 341–350.
(16) Albinati, A.; Bovens, M.; Ruegger, H.; Venanzi, L. M. *Inorg. Chem.* **1997**, *36*, 5991–5999.
(17) Boaretto, R.; Ferrari, A.; Merlin, M.; Sostero, S.; Traverso, O. *J. Photochem. Photobiol. A: Chem.* **2000**, *135*, 179–183.
(18) Boaretto, R.; Paolucci, G.; Sostero, S.; Traverso, O. *J. Mol. Catal A: Chem.* **2003**, *204−205*, 253–258.
(19) Katayama, H.; Yamamura, K.; Miyaki, Y.; Ozawa, F. *Organometallics* **1997**, *16*, 4497–4500.
(20) Trzeciak, A. M.; Ziółkowski, J. *Appl. Organomet. Chem.* **2004**, *18*, 124–129.
(21) Van Rooy, S.; Cao, C.; Patrick, B. O.; Lam, A.; Love, J. A. *Inorg. Chim. Acta* **2006**, *359*, 2918–2923.
(22) Hallett, A. J.; Adams, C. J.; Anderson, K. M.; Baber, R. A.; Connelly, N. G.; Prime, C. J. *Dalton Trans.* **2010**, *39*, 5899–5907.
(23) (a) Carmona, E.; Cingolani, A.; Marchetti, F.; Pettinari, C.; Pettinari, R.; Skelton, B. W.; White, A. H. *Organometallics* **2003**, *22*, 2820–2826. (b) Pettinari, C.; Pettinari, R.; Marchetti, F.; Macchioni, A.; Zuccaccia, D.; Skelton, B. W.; White, A. H. *Inorg. Chem.* **2007**, *46*, 896–906.
(24) Rheingold, A. L.; Yap, G.; Trofimenko, S. *Inorg. Chem.* **1995**, *34*, 759–760.
(25) Craven, E.; Mutlu, E.; Lundberg, D.; Temizedmir, S.; Dechert, S.; Brombacher, H.; Janiak, C. *Polyhedron* **2002**, *21*, 553–562.
(26) Janiak, C.; Temizdemir, S.; Dechert, S.; Deck, W.; Girgsdies, F.; Heinze, J.; Kolm, M. J.; Scharmann, T. G.; Zipffel, O. M. *Eur. J. Inorg. Chem.* **2000**, 1229–1241.
(27) Rheingold, A. L.; Ostrander, R. L.; Haggerty, B. S.; Trofimenko, S. *Inorg. Chem.* **1994**, *33*, 3666–3676.

Chart 1. Proton and Carbon Numbering Scheme for the Tp^{4Bo}, $Tp^{4Bo,5Me}$, Tp^{a-3Me}, and Tp^{a*-3Me} Ligands

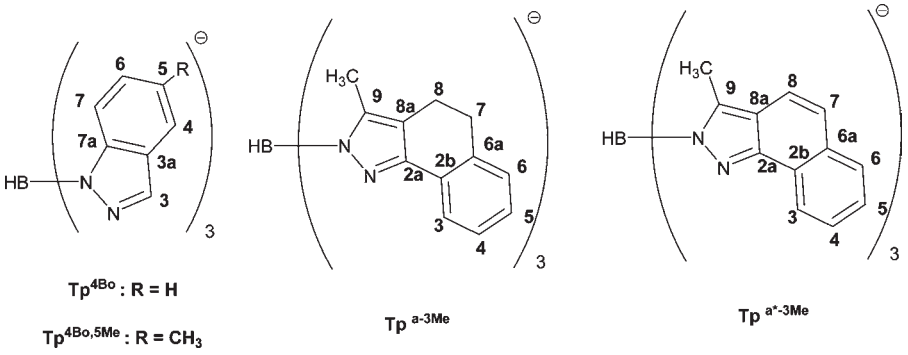

solvents were distilled prior to use. Toluene, tetrahydrofuran (THF), and light petroleum (310−333 K) were dried by refluxing over freshly cut sodium. Other solvents were dried and purified by standard procedures. Salts of the scorpionate ligands Tp, Tp*, Tp^{4Bo}, $Tp^{4Bo,5Me}$, $Tp^{a,3Me}$, $Tp^{a*,3Me}$, were synthesized as previously reported.[9,24−28] The samples for microanalyses were dried in vacuo to constant weight (20 °C, ca. 0.1 Torr). Elemental analyses (C, H, N) were performed in-house with a Fisons Instruments 1108 CHNS-O Elemental Analyzer. IR spectra were recorded from 4000 to 200 cm^{-1} with a Perkin-Elmer Spectrum 100 FT-IR instrument and a Perkin-Elmer System 2000 FT-IR instrument. ^1H, ^{11}B, ^{13}C NMR spectra were recorded on a 400 Mercury Plus Varian instrument operating at room temperature (400 MHz for ^1H and 100 MHz for ^{13}C). ^1H and ^{13}C chemical shifts (δ) are reported in parts per million (ppm) from $SiMe_4$ (^1H and ^{13}C calibration by internal deuterium solvent lock). Abbreviations: ol = olefin; indaz = indazolyl; d = doublet, t = triplet; m = multiplet. Melting points are uncorrected and were taken on an STMP3 Stuart scientific instrument and on a capillary apparatus.

SS NMR Spectroscopy. ^{15}N SS NMR spectra were recorded on a Bruker Avance II 400 instrument operating at 400.23 and 40.55 MHz for ^1H and ^{15}N nuclei, respectively. Cylindrical 4 mm o.d. zirconia rotors with a sample volume of 120 μL were employed and spun at 7 kHz. A ramp cross-polarization pulse sequence was used with a contact time of 4 ms, a ^1H 90° pulse of 3.05 μs, recycle delays of 10−20 s, and 16000−20000 transients. A two pulse phase modulation (TPPM) decoupling scheme was used with an rf field of 75 kHz. ^{15}N chemical shifts were referenced with the resonance of $(NH_4)_2SO_4$ (^{15}N signal at δ = 355.8 ppm with respect to CH_3NO_2).

Computational Details. All calculations were performed with the Gaussian 09 (G09) program package[29] employing the density functional theory (DFT) method with Becke's three parameter hybrid functional[30] and Lee−Yang−Parr's gradient-corrected correlation functional (B3LYP).[31] The Los Alamos double-ζ (LanL2Dz) basis set and effective core potential were used for Rh atoms, and the split-valence 6-31G* basis set was applied for all other atoms. The ground-state geometries of the complexes were optimized in the gas phase. This approximation does not take into account the weak interactions of the solid state, which would require a periodic plane-wave computational approach, but the results appear to be reasonably in agreement with the experimental data, probably because the intermolecular interactions are less pronounced in these neutral complexes.

The nature of all stationary points was confirmed by performing a normal-mode analysis. These geometries were employed for calculations of the absolute magnetic shielding σ, performed at the B3LYP/6-31++G** level using the GIAO method of Gaussian 09. The σ values were converted into ^{15}N chemical shifts δ relative to the magnetic shielding of nitromethane, computed at the same B3LYP/6-31++G** level (σ = −129.5451), taken as reference (experimental 355.8 ppm).

Structure Determinations. Full spheres of CCD area-detector diffractometer data were measured (ω-scans; monochromatic Mo Kα radiation, λ = 0.71073 Å) yielding $N_{t(otal)}$ reflections, these merging to N unique (R_{int} cited) after "empirical"/multiscan absorption correction (proprietary software), these being used in the full matrix least-squares refinements, refining anisotropic displacement parameters for the non-hydrogen atoms, hydrogen atom treatment following a "riding" model; reflection weights were $(\sigma^2(F^2) + (aP)^2 (+ bP))^{-1}$ ($P = (F_o^2+2F_c^2)/3$). Neutral atom complex scattering factors were employed within the SHELXL 97 program.[32] Pertinent results are given in the tables and figures, the latter showing 20% (room-temperature) or 50% (153 or 100 K) probability amplitude displacement envelopes for the non-hydrogen atoms, hydrogen atoms having arbitrary radii of 0.1 Å. Full .cif depositions (excluding structure factor amplitudes) reside with the Cambridge Crystallographic Data Centre, CCDC 682597−682601, 783342. Individual variations in procedure: For **9**, the peripheral atoms of the cod ligand were modeled as disordered over pairs of sites, occupancies set at 0.5 after trial refinement; this structure has been determined previously as an MeCN hemisolvate, non-disordered, in a lattice ($Cmc2_1$, a = 10.815(2), b = 10.127(1), c = 33.316(5) Å) which may be a development of the present. High residuals for **2**·C_4H_8O appear to be consequent on desolvation.

Syntheses of the Complexes. [Rh(cod)Tp^{4Bo}], (1). A toluene solution (10 mL) containing $[Rh(cod)(\mu\text{-}Cl)]_2$ (0.106 g, 0.214 mmol) and $TlTp^{4Bo}$ (0.248 g, 0.436 mmol) was stirred at −10 °C for 3 h. The solvent was then removed under vacuum, and the residue extracted with hexane and filtered to remove TlCl. After solvent evaporation under vacuum, the resulting yellow residue, recrystallized from THF at 4 °C, has been characterized as compound **1** (0.170 g, 0.296 mmol, yield 68%). Mp 270 °C dec Anal. Calcd. for $C_{29}H_{28}BN_6Rh$, C, 60.65; H, 4.91; N, 14.63%.

(28) Trofimenko, S. *Inorg. Synth.* **1970**, *12*, 99–106.
(29) Frisch, M. J.; Trucks, G. W.; Schlegel, H. B.; Scuseria, G. E.; Robb, M. A.; Cheeseman, J. R.; Scalmani, G.; Barone, V.; Mennucci, B.; Petersson, G. A.; Nakatsuji, H.; Caricato, M.; Li, X.; Hratchian, H. P.; Izmaylov, A. F.; Bloino, J.; Zheng, G.; Sonnenberg, J. L.; Hada, M.; Ehara, M.; Toyota, K.; Fukuda, R.; Hasegawa, J.; Ishida, M.; Nakajima, T.; Honda, Y.; Kitao, O.; Nakai, H.; Vreven, T.; Montgomery, J. A. Jr.; Peralta, J. R.; Ogliaro, F.; Bearpark, M.; Heyd, J. J.; Brothers, E.; Kudin, K. N.; Staroverov, V. N.; Kobayashi, R.; Normand, J.; Raghavachari, K.; Rendell, A.; Burant, J. C.; Iyengar, S. S.; Tomasi, J.; Cossi, M.; Rega, N.; Millam, J.; Klene, M.; Knox, J. E.; Cross, J. B.; Bakken, V.; Adamo, C.; Jaramillo, J.; Gomperts, R.; Stratmann, R. E.; Yazyev, O.; Austin, A. J.; Cammi, R.; Pomelli, C.; Ochterski, J.; Martin, R. L.; Morokuma, K.; Zakrzewski, V. G.; Voth, G. A.; Salvador, P.; Dannenberg, J. J.; Dapprich, S.; Daniels, A. D.; Farkas, O.; Foresman, J. B.; Ortiz, J. V.; Cioslowski, J.; Fox, D. J. *Gaussian 09*, Revision A.02; Gaussian, Inc.: Wallingford, CT, 2009.
(30) Becke, A. D. *J. Chem. Phys.* **1993**, *98*, 5648–5652.
(31) Lee, C.; Yang, W.; Parr, R. G. *Phys. Rev. B: Condens. Matter* **1988**, *37*, 785–789.
(32) Sheldrick, G. M. *Acta Crystallogr., Sect. A* **2008**, *64*, 112–122.

Found: C, 60.10; H, 4.97; N, 14.30%. IR (cm^{-1}): 2491sh, 2465 m ν(B−H), 1907w, 1781w, 1673w, ν(C···C), 1619s, 1567 m ν(C···C, C···N), 595s, 432s. ^{1}H NMR ($CDCl_3$, 293 K): δ, 2.01 (m, 4H, H_{endo} (cod)), 2.64 (m, 4H, H_{exo}(cod)), 4.15 (br, 4H_{ol}, H(cod)), 7.07 (m, 3H, H6$_{indaz}$), 7.35 (m, 3H, H5$_{indaz}$), 7.67 (d, 3H, H7$_{indaz}$), 7.89 (d, 3H, H4$_{indaz}$), 8.34 (s, 3H, H3$_{indaz}$). ^{1}H NMR ($CDCl_3$, 323 K): δ, 2.03 (m, 4H, H_{endo} (cod)), 2.69 (m, 4H, H_{exo} (cod)), 4.15 (br, 4H, H(cod)), (br, 1H, B−H), 7.04 (m, 3H, H6$_{indaz}$), 7.31 (m, 3H, H5$_{indaz}$), 7.64 (d, 3H, H7$_{indaz}$), 7.90 (d, 3H, H4$_{indaz}$), 8.31 (s, 3H, H3$_{indaz}$). ^{1}H NMR (THF-d^8, 293 K): δ, 2.05 (m, 4H, H_{endo} (cod)), 2.80 (m, 4H, H_{exo} (cod)), 4.18 (br, 4H, H_{exo} (cod)), 4.76 (br, 1H, B−H), 7.02 (m, 3H, H6$_{indaz}$), 7.32 (m, 3H, H5$_{indaz}$), 7.65 (d, 3H, H7$_{indaz}$), 8.01 (d, 3H, H4$_{indaz}$), 8.45 (s, 3H, H3$_{indaz}$). ^{1}H NMR (THF-d^8, 213 K): δ, 2.05 (d, 4H, H_{endo} (cod)), 2.98 (d, 4H, H_{exo}(cod)), 4.17 (s, 4H, H(cod)), 5.90 (sbr, 1H, B−H), 7.08 (m, 3H, H6$_{indaz}$), 7.40 (m, 3H, H5$_{indaz}$), 7.74 (d, 3H, H7$_{indaz}$), 8.12 (d, 3H, H4$_{indaz}$), 8.62 (s, 3H, H3$_{indaz}$). ^{13}C NMR ($CDCl_3$, 293 K): δ, 31.6 (s, CH_2 (cod)), 75.0 (d, C_{ol} (cod), J(^{103}Rh−^{13}C): 13.6 Hz), 112.3 (s, C6$_{indaz}$), 120.4 (s, C4$_{indaz}$), 120.7 (s, C5$_{indaz}$), 123.6 (s, C3$^a_{indaz}$), 126.6 (s, C7$_{indaz}$), 133.9 (s, C3$_{indaz}$), 143.9 (s, C7$^a_{indaz}$). ^{11}B NMR ($CDCl_3$, 298 K): δ, −8.51.

[Rh(nbd)Tp^{4Bo}], (2). Compound **2** (0.198 g, 0.360 mmol, yield 75%) was prepared following a procedure similar to that reported for **1** by using [Rh(nbd)(μ-Cl)]$_2$ and TlTp^{4Bo}. Mp 282−283 °C. Anal. Calcd. for $C_{28}H_{24}BN_6Rh$, C, 60.24; H, 4.33; N, 15.05%. Found: C, 59.98; H, 4.27; N, 14.91%. IR (cm^{-1}): 2462 ν(B−H), 1619s, 1567 m, 1500s ν(C···C), ν(C···C, C···N). ^{1}H NMR ($CDCl_3$, 293 K): δ, 1.39 (s, 2H, H_{br} (nbd)), 3.50 (m, 4H, H_{ol} (nbd)), 3.93 (sbr, 2H, H_{br} (nbd)), 7.05 (t, 3H, H6$_{indaz}$), 7.34 (t, 3H, H5$_{indaz}$), 7.64 (d, 3H, H7 $_{ndaz}$), 7.98 (d, 3H, H4$_{indaz}$), 8.22 (s, 3H, H3$_{indaz}$). ^{1}H NMR ($CDCl_3$, 273 K): δ, 1.38 (s, 2H, H_{br} (nbd)), 3.52 (m, 4H, H_{ol} (nbd)), 3.94 (sbr, 2H, H_{br} (nbd)), 7.07 (t, 3H, H6$_{indaz}$), 7.37 (t, 3H, H5$_{indaz}$), 7.66 (d, 3H, H7$_{indaz}$), 8.00 (d, 3H, H4$_{indaz}$), 8.25 (s, 3H, H3$_{indaz}$). ^{1}H NMR ($CDCl_3$, 193.2 K): δ, 1.33 (s, 2H, H_{br} (nbd)), 3.46 (s, 4H, H^{ol} (nbd)), 3.94 (s, 2H, H_{brh} (nbd)), 7.04 (t, 3H, H6$_{indaz}$), 7.34 (m, 3H, H5$_{indaz}$), 7.65 (t, 3H, H7 $_{indaz}$), 7.98 (d, 3H, H4$_{indaz}$), 8.26 (s, 3H, H3$_{indaz}$). ^{13}C NMR ($CDCl_3$, 291 K): δ, 38.4 (d, C_{ol} (nbd), J^1(^{103}Rh−^{13}C): 10.0 Hz), 48.0 (d, C_{brh} (nbd), J^2(^{103}Rh−^{13}C): 2.3 Hz), 58.6 (d, C_{br} (nbd), J^3(^{103}Rh−^{13}C): 6.1 Hz), 112.2 (s, C6$_{indaz}$), 120.3 (s, C4$_{indaz}$), 120.6 (s, C5$_{indaz}$), 123.4 (s, C3$^a_{indaz}$), 126.4 (s, C7$_{indaz}$), 134.2 (s, C3$_{indaz}$), 143.6 (s, C7$^a_{indaz}$). ^{11}B NMR ($CDCl_3$, 298 K): δ, −8.73. ^{11}B NMR (THF-d^8, 298 K): δ, −8.72.

[Rh(cod)Tp^{4Bo,5Me}], (3). Compound **3** (0.219 g, 0.345 mmol, yield 68%) was prepared following a procedure similar to that reported for **1** by using [Rh(cod)(μ-Cl)]$_2$ and TlTp^{4Bo,5Me}. Mp 104−105 °C. Anal. Calcd. for $C_{32}H_{34}BN_6Rh$, C, 62.36; H, 5.56; N, 13.63%. Found: C, 62.08; H, 5.62; N, 13.28%. IR (cm^{-1}): 2500sh, 2482 m ν(B−H), 1626s, 1567w, 1510s ν(C···C, C···N), 586s, 464 m, 430s, 380 m. ^{1}H NMR (THF-d^8, 293 K): δ, 2.03 (m, 4H, H_{endo} (cod)), 2.36 (s, 9H, CH_{3indaz}), 2.78 (m, 4H, H_{exo} (cod)), 4.18 (br, 4H, H_{ol} (cod)), 4.78 (br, 1H, B−H), 7.16 (d, 3H, H6$_{indaz}$), 7.39 (s, 3H, H4$_{indaz}$), 7.85 (d, 3H, H7$_{indaz}$), 8.31 (s, 3H, H3$_{indaz}$). ^{1}H NMR (CD_2Cl_2, 298 K): δ, 2.02 (m, 4H, H_{endo} (cod)), 2.40 (s, 9H, CH_{3indaz}), 2.64 (m, 4H, H_{exo} (cod)), 4.12 (br, 4H, H_{ol} (cod)), 7.19 (d, 3H, H6$_{indaz}$), 7.43 (s, 3H, H4$_{indaz}$), 7.81 (d, 3H, H7$_{indaz}$), 8.25 (s, 3H, H3$_{indaz}$). ^{1}H NMR (CD_2Cl_2, 193 K): δ, 1.96 (m, 4H, H_{endo} (cod)), 2.34 (s, 9H, CH_{3indaz}), 2.68 (m, 4H, H_{exo} (cod)), 4.01 (br, 4H, H_{ol} (cod)), 7.19 (d, 3H, H6$_{indaz}$), 7.38 (s, 3H, H4$_{indaz}$), 7.84 (d, 3H, H7$_{indaz}$), 8.27 (s, 3H, H3$_{indaz}$). ^{13}C NMR (THF-d^8, 293 K): δ, 21.4 (CH_{3indaz}), 32.2 (CH_2 (cod)), 74.7 (d, C_{ol} (cod), J(^{103}Rh−^{13}C): 13.9 Hz), 112.5 (s, C6$_{indaz}$), 119.6 (s, C5$_{indaz}$), 123.8 (s, C3$^a_{indaz}$), 129.2 (s, C7$_{indaz}$), 130.3 (s, C4$_{indaz}$), 133.7 (s, C3$_{indaz}$), 142.3 (s, C7$^a_{indaz}$). ^{11}B NMR ($CDCl_3$, 298 K): δ, −8.86.

[Rh(nbd)Tp^{4Bo,5Me}], (4). Compound **4** (0.174 g, 0.303 mmol, yield 70%) was prepared following a procedure similar to that reported for **1** by using [Rh(nbd)(μ-Cl)]$_2$ and TlTp^{4Bo,5Me}. Mp 255 °C dec Anal. Calcd. for $C_{31}H_{30}BN_6Rh$, C, 62.02; H, 5.04; N, 14.00%. Found: C, 62.21; H, 5.19; N, 13.84%. IR (cm^{-1}): 2472 m ν(B−H), 1627s, 1602 m, 1567w, 1509s ν(C···C, C···N). ^{1}H NMR ($CDCl_3$, 293 K): δ, 1.36 (m, 2H, H_{br} (nbd)), 2.39 (s, 9H, CH_{3indaz}), 3.50 (m, 4H, H_{ol} (nbd)), 3.95 (m, 2H, H_{br} (nbd)), 7.14 (d, 3H, H6$_{indaz}$), 7.37 (s, 3H, H4$_{indaz}$), 7.84 (d, 3H, H7$_{indaz}$), 8.09 (s, 3H, H3$_{indaz}$). ^{13}C NMR ($CDCl_3$, 293 K): δ, 21.6 (s, CH_{3indaz}), 38.1 (d, C_{ol} (nbd), J^1(^{103}Rh−^{13}C): 10.6 Hz), 48.0 (d, C_{brh} (nbd), J^2(^{103}Rh−^{13}C): 2.2 Hz), 58.6 (d, H_{br} (nbd), J^3(^{103}Rh−^{13}C): 6.4 Hz), 111.9 (s, C6$_{indaz}$), 118.9 (s, C5$_{indaz}$), 123.7 (s, C3$^a_{indaz}$), 128.6 (s, C7$_{indaz}$), 129.8 (s, C4$_{indaz}$), 133.4 (s, C3$_{indaz}$), 142.4 (s, C7$^a_{indaz}$). ^{11}B NMR (THF-d^8, 298 K): δ, −8.70.

[Rh(cod)Tp^{a,3Me}], (5). Compound **5** (0.112 g, 0.145 mmol, yield 60%) was prepared following a procedure similar to that reported for **1** by using [Rh(cod)(μ-Cl)]$_2$ and TlTp^{a,3Me}. Mp 210 °C. Anal. Calcd. for $C_{44}H_{46}BN_6Rh$, C, 68.40; H, 6.00; N, 10.88%. Found: C, 67.99; H, 5.95; N, 10.77%. IR (cm^{-1}): 2463 m ν(B−H), 1605 m, 1580w, 1557 m, 1537s ν(C···C, C···N), 609w, 542w, 482w, 390w. ^{1}H NMR ($CDCl_3$, 293 K): δ, 1.70, 1.90 (s, 4H, H_{endo}), 2.36 (s, 3H, CH_3), 2.43 (s, 6H, CH_3), 2.74 (s br, 6H, CH_2), 2.84 (s br, 10H, 6H−CH_2 and 4H_{cod}), 3.80, 4.17 (br, 4H, H_{ol}), 4.80 (s, 1H, B−H), 7.26 (s br, 6H, H3, H4, H5), 7.50 (s br, 3H, H3, H4, H5), 7.91(s br, 1H, H6), 9.54 (d, 2H, H6). ^{13}C NMR ($CDCl_3$, 293 K): δ, 10.9, 12.2 (s, CH_3), 19.7, 18.8, 29.1, 30.5 (s, CH_2 (Tp^{a,3Me}) + CH_2 (cod)), 80.2 (d br, C_{ol} (cod)), 116.9, 117.2 (s, C4), 122.1, 125.4, 125.7, 127.5, 128.0, 128.4 129.1, 129.1, 137.2, 137.8 (s, C8^a), 142.6 (s, C2^a), 148.2, 148.8 (s, C9).

[Rh(nbd)Tp^{a,3Me}], (6). Compound **6** (0.127 g, 0.168 mmol, yield 61%) was prepared following a procedure similar to that reported for **1** by using [Rh(nbd)(μ-Cl)]$_2$ and TlTp^{a,3Me}. Mp 252 °C. Anal. Calcd. for $C_{43}H_{42}BN_6Rh$, C, 68.27; H, 5.60; N, 11.11%. Found: C, 68.07; H, 5.50; N, 11.04%. IR (cm^{-1}): 2437mbr ν(B−H), 1620 m, 11582w, 1556w ν(C···C, C···N). ^{1}H NMR ($CDCl_3$, 293 K): 0.80 (s, 2H, H_{br} (nbd)), 2.21 (s, 9H, CH_3), 2.64 (t, 6H, CH_2), 2.94 (t, 6H, CH_2), 3.21 (s, 2H, H_{brh} (nbd)), 3.65 (s, 4H, H_{ol} (nbd)), 7.22, 7.48 (m, 9H, H3, H4, H5), 8.90 (d, 3H, H6). ^{13}C NMR ($CDCl_3$, 293 K): δ, 11.5 (s, CH_3), 19.6, 30.6 (s, CH_2, Tp^{a,3Me}), 50.0 (d, C_{brh} (nbd), J^2(^{103}Rh−^{13}C): 3.0 Hz), 58.2 (d, C^{ol} (nbd), J^1(^{103}Rh−^{13}C): 9.9 Hz), 62.8 (d, C_{br} (nbd), J^3(^{103}Rh−^{13}C): 6.1 Hz), 116.2 (s, C4), 124.2, 126.4, 127.1, 128.3, 130.2, 137.6 (s, C8^a), 140.8 (s, C2^a), 148.6 (s, C9).

[Rh(cod)Tp^{a*,3Me}], (7). Compound **7** (0.112 g, 0.145 mmol, yield 60%) was prepared following a procedure similar to that reported for **1** by using [Rh(cod)(μ-Cl)]$_2$ and TlTp^{a*,3Me}. Mp 210 °C. Anal. Calcd. for $C_{44}H_{46}BN_6Rh$, C, 68.40; H, 6.00; N, 10.88%. Found: C, 67.99; H, 5.95; N, 10.77%. IR (cm^{-1}): 2463 m ν(B−H), 1605 m, 1580w, 1557 m, 1537s ν(C···C, C···N), 609w, 542w, 482w, 390w. ^{1}H NMR ($CDCl_3$, 293 K): δ, 1.70, 1.90 (s, 4H, H_{endo}), 2.36 (s, 3H, CH_3), 2.43 (s, 6H, CH_3), 2.74 (sbr, 6H, CH_2), 2.84 (sbr, 10H, 6H−CH_2 and 4H−COD), 3.80, 4.17 (br, 4H, H_{ol}), 4.80 (s, 1H, B−H), 7.26 (sbr, 6H, H3, H4, H5), 7.50 (sbr, 3H, H3, H4, H5), 7.91(sbr, 1H, H6), 9.54 (d, 2H, H6). ^{13}C NMR ($CDCl_3$, 293 K): δ, 10.6, 11.3, 12.3, 12.7, 13.8 (s, CH_3), 21.7, 28.2, 28.8, 29.4, 29.9, 30.2, 31.1 (s, CH_2 Tp^{a*,3Me} and CH_2 (cod)), 80.1, 81.4 (sbr, C_{ol} (cod)), 80.8, 81.0 (s, C_{ol} (cod)), 85.9, 88.0 (s, C_{ol} (cod)), 132.5, 133.8, 134.07, 134.3, 135.8, 138.1 (s, C8^a), 142.9, 143.5 (s, C2^a),145.6, 147.0, 147.2 (s, C9).

[Rh(nbd)Tp^{a*,3Me}], (8). Compound **8** (0.132 g, 0.176 mmol, yield 50%) was prepared following a procedure similar to that reported for **1** by using [Rh(nbd)(μ-Cl)]$_2$ and TlTp^{a*,3Me}. Mp 194−204 °C. Anal. Calc. for $C_{43}H_{36}BN_6Rh$, C, 68.82; H, 4.83; N, 11.20%. Found: C, 68.40; H, 5.42; N, 10.24%. IR (cm^{-1}): 2470 m ν(B−H), 1629s, 1613 m, 1555w ν(C···C, C···N). ^{1}H NMR ($CDCl_3$, 293 K): 0.70, 0.76 (s, 2H, H_{br} (nbd)), 2.37 (s, 3H, CH_3), 2.53 (s, 6H, CH_3), 2.69 (s, 9H, CH_3), 2.80−2.90 (sbr, 2H, H_{brh} (nbd)), 3.76, 3.82 (s, 4H, H_{ol} (nbd)), 7.17−7.36 (m, 6H, H3, H4, H5), 7.49−7.85 (sbr, 3H, H3, H4, H5), 9.44, 9.75 (d, 3H, H6). ^{13}C NMR ($CDCl_3$, 293 K): δ, 11.5, 11.9, 13.3 (s, CH_3), 50.4 and 50.0 (d, C_{brh} (nbd), J^2(^{103}Rh−^{13}C): 2.6 Hz), 59.1, 59.3, 59.5 (d, C_{ol} (nbd), J^1(^{103}Rh−^{13}C): 9.0 Hz), 63.0, 63.2 and 63.4, 63.6 (d,

Chart 2

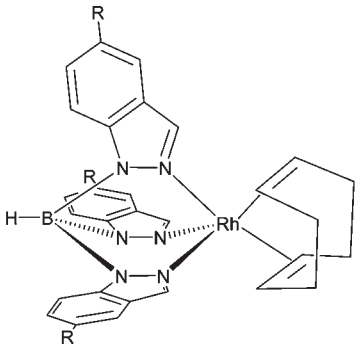

1, R = H, $Tp^x = Tp^{4Bo}$
3, R = CH_3, $Tp^x = Tp^{4Bo,5Me}$

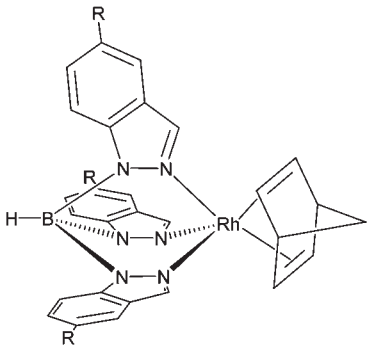

2, R = H, $Tp^x = Tp^{4Bo}$
4, R = CH_3, $Tp^x = Tp^{4Bo,5Me}$

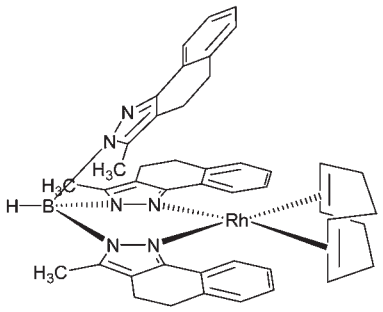

5, $Tp^x = Tp^{a\text{-}3Me}$

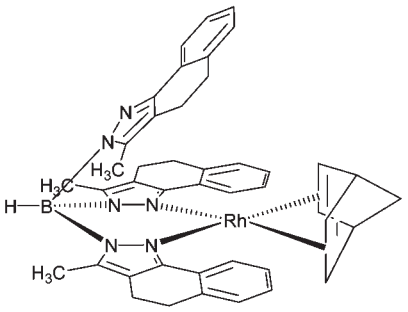

6, $Tp^x = Tp^{a\text{-}3Me}$

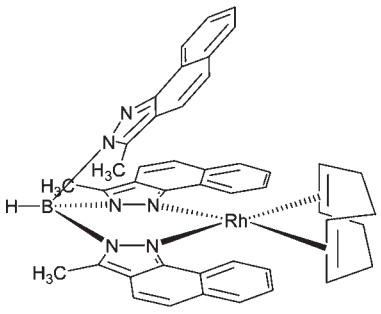

7, $Tp^x = Tp^{a*\text{-}3Me}$

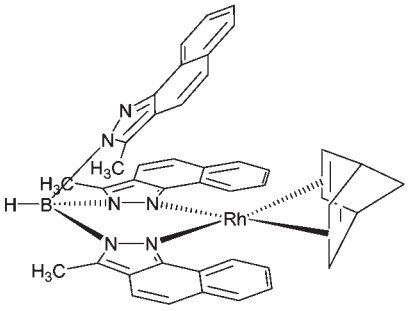

8, $Tp^x = Tp^{a*\text{-}3Me}$

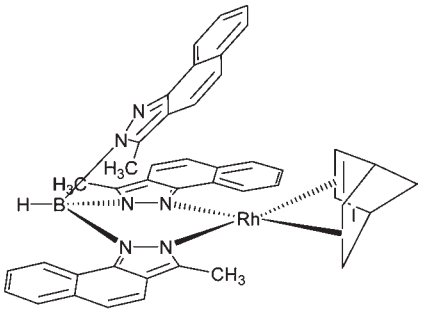

8*, $Tp^x = Tp^{a*\text{-}3Me*}$

C_{br} (nbd), $J^3(^{103}Rh-^{13}C)$: 6.4 Hz), 117.8, 119.2, 119.3, 119.5, 119.7, 121.4, 121.8, 123.0, 123.6, 123.8, 124.8, 125.4, 125.7, 125.8, 126.1, 126.3, 126.5, 126.6, 128.3, 128.4, 129.2, 133.3, 133.5, 134.4 (s, $C8^a$), 139.2, 140.1 (s, $C2^a$), 147.1, 147.2 (s, C9).

Complexes [Rh(cod)Tp] (**9**), [Rh(nbd)Tp] (**10**), [Rh(cod)Tp*] (**11**), and [Rh(nbd)Tp*] (**12**) were prepared following a similar procedure but using the appropriate $[Rh(diene)(\mu\text{-}Cl)]_2$ dimer and the corresponding $MTp^{x\prime}$ (M = Na, K, or Tl) salts as reagents. Their analytical and spectral data are in accordance with those reported in the literature.[12]

Results and Discussion

Synthesis of Complexes 1−12. The complexes [Rh(diene)Tp^x] (Chart 2) ($Tp^x = Tp^{4Bo}$, diene = cod, **1**; nbd, **2**; **3**: $Tp^x = Tp^{4Bo,5Me}$, diene = cod, **3**; nbd, **4**; $Tp^x = Tp^{a,3Me}$, diene = cod, **5**; nbd, **6**; $Tp^x = Tp^{a*,3Me}$, diene = cod, **7**; nbd, **8**; Tp^x = Tp, diene = cod, **9**; nbd, **10**; Tp^x = Tp*, diene = cod, **11**; nbd, **12**) have been prepared from the reactions of equimolar quantities of $[Rh(diene)(\mu\text{-}Cl)]_2$ dimers and tris(pyrazolyl)borate salts M[Tp^x], in toluene, under N_2 streams. Tl[Tp^x] can be efficiently used in place of potassium salts. The products are red to orange air-stable solids that are soluble in $CHCl_3$, CH_2Cl_2, THF, MeCN, and hexane. It is noteworthy that the formation of compound **8** is accompanied by that of a small amount of [Rh(nbd)$Tp^{a*,3Me*}$], **8***, because of a 1,2-borotropic rearrangement of one of the pyrazolyl donors, as previously observed also in complexes of the type [Ir(cod)Tp^x].[16] Complexes **2**, **3**, **6**, **8.8***, **8***, and **9** were fully characterized by X-ray crystallography (Table 1).

Structural Studies. In each of the single crystal X-ray studies undertaken, one formula unit, devoid of crystallographic symmetry and comprising a mononuclear neutral molecule (accompanied by thf solvent in the cases of **2** and **3**), comprises the asymmetric unit of the structure (exception: the complex **8.8*** (an Et_2O disolvate) has one neutral mononuclear molecule of each type comprising the asymmetric unit). In each case the molecule consists of a rhodium atom, coordinated ("chelated") by a diene

Table 1. Crystal/Refinement Data

	[Rh(nbd)Tp^{4Bo}].thf	[Rh(cod)Tp^{4Bo,5Me}].2thf	[Rh(nbd)Tp^{a,3Me}]	[Rh(nbd)Tp^{a*,3Me}]	[Rh(nbd)Tp^{a*,3Me*}]	[Rh(cod)Tp]
	2·C_4H_8O	**3**·2C_4H_8O	**6**	**8.8***·2Et_2O	**8***	**9**
formula	$C_{32}H_{32}BN_6ORh$	$C_{40}H_{50}BN_6O_2Rh$	$C_{43}H_{42}BN_6Rh$	$C_{94}H_{92}B_2N_{12}O_2Rh_2$	$C_{43}H_{36}BN_6Rh$	$C_{17}H_{22}BN_6Rh$
M_r (Dalton)	630.4	760.6	756.6	1649.2	750.5	424.1
cryst syst	monoclinic	monoclinic	monoclinic	triclinic	triclinic	triclinic
space group	$P2_1$ (#4)[a]	$C2/c$ (#15)	$P2_1/c$ (#14)	$P\bar{1}$ (#2)	$P\bar{1}$ (#2)	$P\bar{1}$ (#2)
a (Å)	9.541(4)	29.341(5)	8.913(1)	13.6255(3)	10.9306(10)	7.2506(7)
b (Å)	10.734(4)	23.010(4)	20.434(3)	14.9316(3)	11.2265(10)	7.5215(8)
c (Å)	14.070(6)	11.700(2)	20.165(3)	21.0256(4)	15.5737(14)	15.866(2)
α (deg)				87.865(2)	71.200(1)	103.512(2)
β (deg)	109.289(5)	112.074(3)	98.430(3)	85.610(2)	82.150(1)	92.130(2)
γ (deg)				65.513(2)	81.685(1)	93.378(2)
V (Å^3)	1360	7320	3633	3881	1782	$836._7$
D_c (g cm^{-3})	1.53_9	1.38_0	1.38_3	1.41_1	1.39_9	1.67_9
Z (f.u.)	2	8	4	2	2	2
μ_{Mo}(mm-1)	0.67	0.51	0.51	0.49	0.52	1.03
specimen (mm)	0.64,0.14,0.03	0.36,0.28,0.17	0.18,0.15,0.14	0.49,0.30,0.11	0.28,0.25,0.24	0.24,0.13,0.12
'T'$_{min/max}$	0.60	0.73	0.93	0.88	0.93	0.83
$2\theta_{max}$ (deg)	55	50	58	74	55	75
N_t	11456	48708	32903	132902	15815	16512
$N(R_{int})$	5861 (0.067)	6449 (0.094)	9039 (0.071)	38578(0.056)	8066 (0.018)	8596 (0.020)
N_o ($I > 2\sigma(I)$)	4761	4492	5030	27575	6296	7696
$R1$	0.090	0.071	0.061	0.038	0.038	0.038
$wR2$ (a,b)	0.23(0.00,24.0)	0.22(0.127,5.4)	0.15(0.057,4.6)	0.100(0.053,0.00)	0.099(0.050,0.37)	0.096(0.048,0.69)
S	1.17	1.18	1.01	0.98	1.06	1.11
T (K)	153	153	298	100	298	153

[a] x_{abs} = 0.34(9).

ligand, and a Tp^x ligand. The compounds fall into two classes, depending on whether the latter is bi- or tridentate, presumably influenced by steric effects of methyl substituents and ring system extensions on the ligand. The former leads to a situation obviously involving a planar "four-coordinate" metal atom environment, as is more usually associated with Rh(I). Our discussion is initially focused on these complexes (**6**, **8**). For both complexes, the nature of the ligand should initially be addressed, in establishing the nature of each compound. In **6** and **8** all borane substituents are identical and identically attached to the boron atom. However, in **8***, where again all borane substituents are identical, their attachment mode to the boron atom differs in respect of the nitrogen atom involved, and coordination to the rhodium atom takes place diversely through one ring system of each type (Figure 2). In this way the potential 3-symmetry of the uncoordinated ligand (which, presumably, was an (interesting) impurity in the bulk homoscorpionate) is lost. In both complexes **6** and **8**, nbd is the diene ligand; metal atom environments are presented comparatively in Table 2.

In **6**, [Rh(ndb)Tp^{a,3Me}], and **8**, [Rh(ndb)Tp^{a*,3Me}], distances and angles are very similar to those already established in other structurally defined complexes of the Rh(ndb) moiety with κ^2-poly pyrazolylborate ligands,[7b,8,12,15] and, ignoring the uncoordinated pendant, the geometry is a very fair approximation to mirror-symmetry (Supporting Information, Figure S1), the maximum difference in any pair of "equivalent" angles not exceeding 3.6°. In **8***, [Rh(nbd)-Tp^{a*,3Me}], the achievement of mirror-symmetry is not possible, and several large divergences in "equivalent" angles are found, concomitant with the asymmetry in the aspects of the donor ring systems (Figure 2).

In **2**, **3**, and **9**, all donor systems within each ligand are similar, and the ligands are tridentate; the metal atom environment within each complex again has quasi mirror-symmetry, broken in the case of the cod complex **3** by the "chirality" of the cod ligand, the latter in **9** being disordered (in quasi-m fashion) over both possibilities. The geometries of **2**, **3**, and **9** (together with those of the previously determined solvate of the latter) are presented in Table 3, wherein the geometry of **2** (Figure 3) may be compared with that of **6** in Table 2. Table 3 shows an asymmetry in the distances Rh−C(1,2), cf. Rh−C(5,6), reproduced also in the (more precisely determined) cod complexes **3** and **9** (Supporting Information, Figure S2, Figure 4), ascribed to the difference in ambience of the diene group vis-à-vis the coordinated nitrogen atoms, that is, C(5,6) vis-à-vis N(2), cf. that of C(1,2) vis-à-vis N(12,32). Considering these in relation to the Rh−C distances, one may ascribe Rh−N(12,32),C(1,2) as "long" and Rh−C(5,6),N(22) as "short", the array C(1,2), C(5,6), N(12,32), N(22) (considering certain atoms pairwise) constituting a redefinition of the "four-coordinate, planar" array (Figure 4). The contacts between the pyrazolate and diene hydrogen atoms lie snugly around the van der Waals limit. In **8.8***, differences in the coordination spheres of the two molecules are most evident in the angular parameters of Table 2, and in the deviation of the rhodium atoms from the $C_{11}N_2$ ligand planes, these being 0.624(2), 0.563(2) Å for **8** and 0.766(2) and 0.012(2) Å for the regular and anomalous donors of **8*** (0.578(2), 0.148(2) Å in the pure **8*** material). Rh−N,C(cod) distances in general are in good agreement with those reported in similar complexes.[6,9,10]

Spectroscopic Characterization of 1−12. Complexes **1−12** were also characterized by elemental analysis, IR spectroscopy, and ^{1}H, ^{13}C, and ^{11}B NMR spectroscopy. The B−H stretching frequencies in the IR spectra and the chemical shifts in the ^{11}B NMR data (Table 4) have been used in several cases to distinguish between κ^2 and κ^3 coordination of the hydridotris(pyrazolyl)borate ligands. The IR spectra of all complexes confirm that the ν(B−H), which fall in the range 2500−2463 cm^{-1}, are mainly

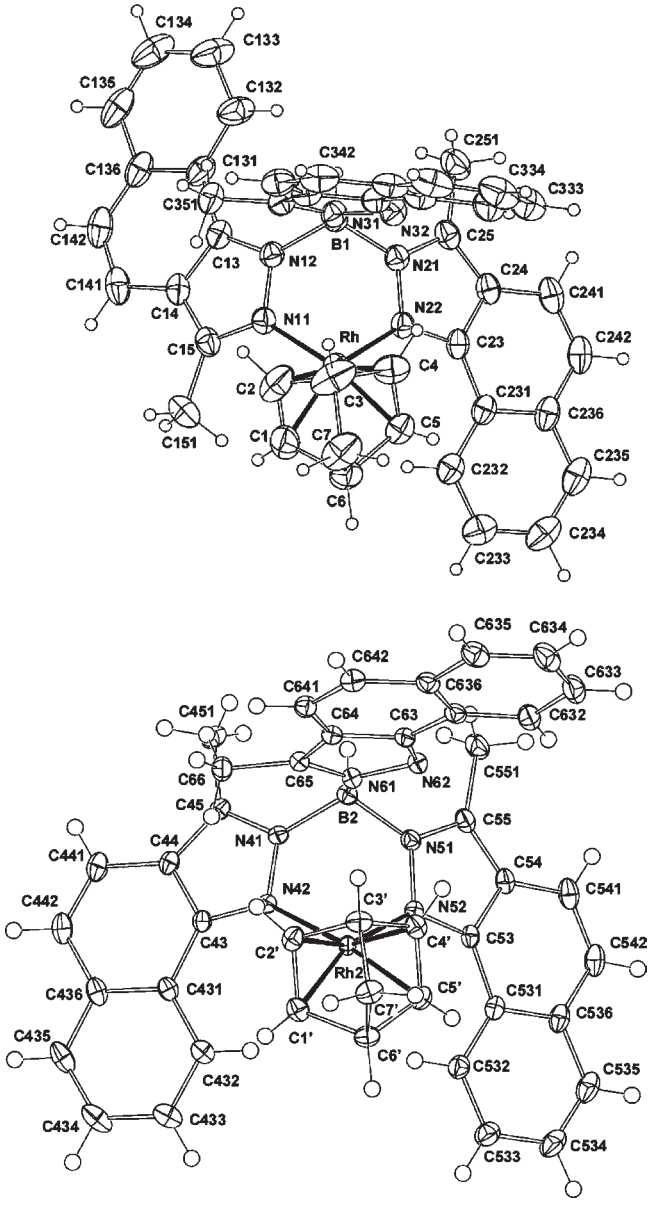

Figure 2. Molecular projections of the two components of **8.8*** · $2Et_2O$ note the difference in attachment of the pendant ring systems of the ligand to the boron atom, and, in consequence, to the rhodium, and the resultant asymmetry in the coordination environment.

influenced by the nature of the substituents on the pz rings. In fact, in the spectra of the cod complexes **5** and **7**, the ν(B−H) at about 2463 cm^{-1} (powder) are consistent with κ^2 coordination in the solid state, as previously established for other [Rh(cod)Tp^x] derivatives.[15] By contrast, complexes **2** and **3** containing the less sterically hindered Tp^{4Bo} and $Tp^{4Bo,5Me}$ ligands, and showing κ^3-coordination as established by the X-ray data, exhibit the ν(BH) at about 2462 and 2482 cm^{-1} (powder) typical of κ^2-coordinated pyrazolylborate ligands. These values agree well with those found for other structurally characterized Tp^{4Bo} complexes containing a κ^3-coordinated scorpionate.[26]

The ^{11}B NMR spectra were recorded for compounds **1**−**4** in $CDCl_3$ solution. For comparison purposes we recorded the ^{11}B spectra of complexes **9**−**12** in the same solvent; these are presented in Table 4, together with data

Table 2. Selected Geometries, [Rh(nbd)$Tp^{a,3Me/a*3Me/a*,3Me*}$] (**6**; **8.8*** · $2Et_2O$; **8***)

atoms	**6**	**8.8*** (two components); **8***[a]
	Distances (Å)	
Rh−C(1)	2.125(5)	2.158(1), 2.138(2); 2.130(3)
Rh−C(2)	2.124(5)	2.125(2), 2.130(2); 2.117(3)
Rh−C(4)	2.135(5)	2.110(1), 2.128(2); 2.130(3)
Rh−C(5)	2.126(5)	2.138(1), 2.142(2); 2.144(3)
Rh−N(12)	2.077(4)	2.106(1), 2.099(1); 2.116(2)
Rh−N(22)	2.104(4)	2.077(1), 2.085(1); 2.086(2)
C(1)−C(2)	1.371(7)	1.390(2), 1.395(2); 1.355(5)
C(4)−C(5)	1.359(7)	1.398(2), 1.395(2); 1.375(4)
	Angles (degrees)	
C(1)−Rh−C(2)	37.7(2)	37.87(6), 38.16(6); 37.2(2)
C(1)−Rh−C(4)	79.2(2)	79.78(6), 79.67(6); 78.6(1)
C(1)−Rh−C(5)	67.0(2)	66.74(6), 66.94(6); 66.4(1)
C(1)−Rh−N(12)	102.5(2)	108.03(6), 107.84(6); 106.7(1)
C(1)−Rh−N(22)	165.3(2)	162.44(5), 153.04(6); 157.9(1)
C(2)−Rh−C(4)	66.7(2)	67.47(6), 67.08(6); 66.4(2)
C(2)−Rh−C(5)	79.1(2)	80.00(6), 79.95(6); 78.9(1)
C(2)−Rh−N(12)	101.4(2)	97.97(5), 99.97(6); 99.9(1)
C(2)−Rh−N(22)	154.9(2)	155.60(6), 165.80(6); 162.1(1)
C(4)−Rh−C(5)	37.2(2)	38.41(6), 38.14(6); 37.5(1)
C(4)−Rh−N(12)	158.5(2)	146.04(5), 149.30(5); 150.5(1)
C(4)−Rh−N(22)	100.1(2)	97.44(5), 102.67(6); 102.2(1)
C(5)−Rh−N(12)	162.3(2)	173.69(5), 171.65(5); 170.22(9)
C(5)−Rh−N(22)	103.5(2)	100.29(5), 98.07(5); 100.53(9)
N(12)−Rh−N(22)	83.7(2)	84.05(5), 84.03(5); 83.63(7)

[a] In **8***, for N(12) read N(11).

Table 3. Selected Geometries, [Rh(nbd)Tp^{4Bo}]; [Rh(cod)$Tp^{4Bo,5Me}$,Tp] (**2**; **3**, **9**; **9** · 0.5MeCN)

atoms	**2**[a]	**3**	**9**; **9** · 0.5MeCN (mols 1,2)[b]
		Distances (Å)	
Rh−C(1)	2.19(2)	2.141(7)	2.155(2); 2.147(5), 2.066(6)
Rh−C(2)	2.13(1)	2.138(6)	2.151(2)
Rh−C(5)	2.03(2)	2.090(6)	2.071(2); 2.064(6), 2.165(6)
Rh−C(6)	2.06(1)	2.060(6)	2.062(2)
Rh−N(12)	2.18(1)	2.252(5)	2.248(2); 2.251(5), 2.245(5)
Rh−N(22)	2.09(1)	2.076(5)	2.092(2); 2.114(7), 2.093(7)
Rh−N(32)	2.19(1)	2.245(5)	2.263(2)
C(1)−C(2)	1.37(2)	1.339(10)	1.381(3); 1.37(1), 1.40(1)
C(5)−C(6)	1.42(2)	1.437(9)	1.424(3); 1.43(1), 1.42(1)
		Angles (degrees)	
C(1)−Rh−C(2)	37.1(6)	36.5(3)	37.42(8); 37.3(3), 37.8(3)
C(1)−Rh−C(5)	78.2(8)	88.9(2)	93.23(9); 92.3(2), 93.7(2)
C(1)−Rh−C(6)	65.1(6)	80.6(2)	80.81(8); 79.6(2), 80.9(2)
C(1)−Rh−N(12)	92.6(7)	88.0(2)	85.09(7); 86.5(2), 85.5(2)
C(1)−Rh−N(22)	153.7(5)	165.7(2)	161.14(8); 161.0(2), 161.0(2)
C(1)−Rh−N(32)	120.5(5)	109.3(2)	110.42(7); 110.9(2), 110.1(2)
C(2)−Rh−C(5)	66.2(6)	80.8(2)	80.57(9)
C(2)−Rh−C(6)	79.9(5)	97.1(2)	93.55(8)
C(2)−Rh−N(12)	115.5(4)	111.3(2)	110.09(8)
C(2)−Rh−N(22)	158.5(4)	157.3(2)	161.04(8)
C(2)−Rh−N(32)	93.9(4)	84.0(2)	86.75(7)
C(5)−Rh−C(6)	40.8(6)	40.5(2)	40.30(9); 40.4(4), 40.2(4)
C(5)−Rh−N(12)	160.8(6)	152.6(2)	157.31(7); 158.4(2), 158.5(2)
C(5)−Rh−N(22)	95.4(5)	91.5(2)	90.60(8); 90.9(2), 90.7(2)
C(5)−Rh−N(32)	118.0(5)	122.9(2)	120.23(8); 118.6(2), 118.8(2)
C(6)−Rh−N(12)	120.0(5)	112.3(2)	117.44(7)
C(6)−Rh−N(22)	93.2(5)	90.5(2)	90.35(7)
C(6)−Rh−N(32)	158.6(5)	162.0(2)	159.70(8)
N(12)−Rh−N(22)	85.5(5)	85.1(2)	84.28(6); 83.7(2), 81.3(2)
N(12)−Rh−N(32)	81.3(4)	83.6(2)	81.18(6); 81.3(2), 81.7(2)
N(22)−Rh−N(32)	85.2(4)	82.3(2)	83.25(6)

[a] For C(5,6) read C(4,5). [b] Data for counterpart values from ref 12. There are two independent molecules in the structure, each disposed about a crystallographic mirror plane.

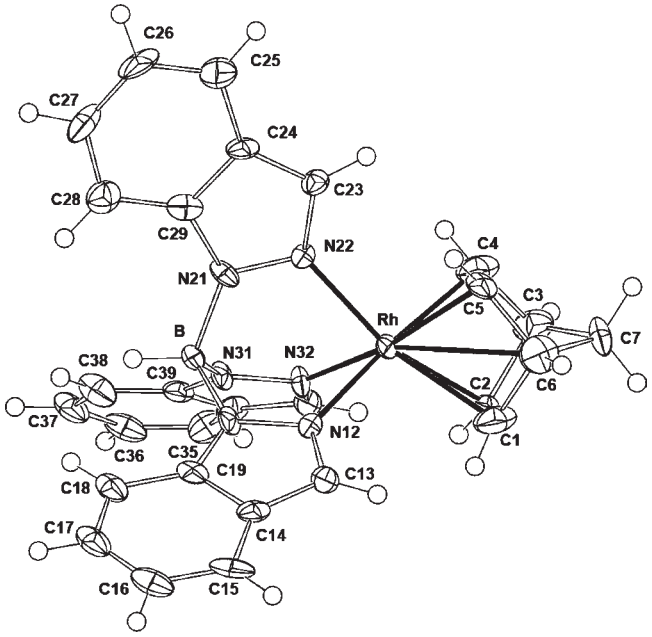

Figure 3. Molecular projection of **2**.

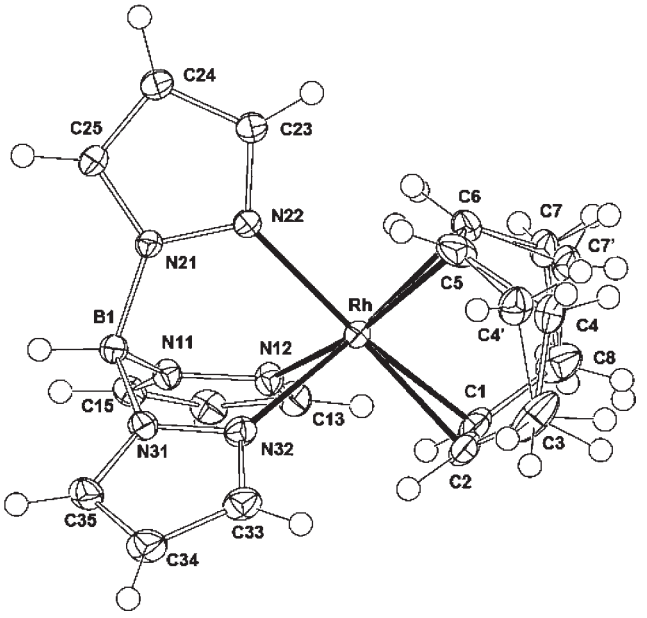

Figure 4. Molecular projection of **9**, oriented to display the "quasi-four-coordinate planar" array in the plane of the page; the cod ligand is disordered.

from ref 13. It has been previously indicated that ^{11}B chemical shifts of Tp^x show the general pattern $\kappa^3 < -7.5$ ppm $< \kappa^2$.[33] The ^{11}B data for **1**−**4** appear consistent with results from the IR and X-ray work, their δ values being in the range −8.51 to −8.86, typical of κ^3-coordination. However this empirical rule seems not to apply for complexes of the unsubstituted Tp which exhibit values typical of κ^2 coordination contrary to the X-ray results, as previously also noted by Adams et al. who recorded analogous spectra in CD_2Cl_2.[12]

(33) Nortchutt, T. O.; Lachicotte, R. J.; Jones, W. D. *Organometallics* **1998**, *17*, 5148–5152.

Table 4. ^{11}B NMR data ($CDCl_3$) of Rhodium Complexes

compound	^{11}B	compound	^{11}B
[Rh(cod)Tp^{4Bo}] (**1**)	−8.51	[Rh(nbd)Tp^{4Bo}] (**2**)	−8.72
[Rh(cod)Tp^{4Bo,5Me}] (**3**)	−8.86	[Rh(nbd)Tp^{4Bo,5Me}] (**4**)	−8.70
[Rh(cod)Tp] (**9**)	−3.59	[Rh(nbd)Tp] (**10**)	−3.60
[Rh(cod)Tp*] (**11**)	−6.19	[Rh(nbd)Tp*] (**12**)	−9.3
[Rh(cod)Tp^{iPr,4Br}][13]	−2.2	[Rh(nbd)Tp^{iPr,4Br}][13]	−2.3
[Rh(cod)Tp^{Me}][13]	−2.0	[Rh(nbd)Tp^{Me}][13]	−3.1

The proton and carbon NMR spectra of complexes **1**−**4**, recorded in $CDCl_3$ or in THF-d^8, indicate in each case the presence of equivalent azolyl rings: the equivalence could be explained as corresponding to a fast motion involving coordinated azolyl (and olefin) groups between the axial and the equatorial sites of the trigonal bipyramidal structure found in the solid state. The existence of four-coordinate Rh centers in solution in the case of **1**−**4** can be excluded on the basis of the ^{13}C chemical shifts of the nbd and cod complexes.[16] The $^{13}C_{diene}$ δ of four- and five-coordinate complexes differ significantly as the electron density at the metal center is higher when the Tp^x is coordinated to the metal in a κ^3 rather than in a κ^2 fashion. The $^{13}C_{diene}$ δ values found for **1**−**4** are in accordance with expectations for five-coordinate rhodium centers.

Complexes **5**−**8** show a different behavior since their δ values related to $^{13}C_{diene}$ are typical of four-coordinated centers.[12,16] Large substituents in the 3-position of the azolyl rings, in fact, should inhibit the formation of five-coordinate (**C** form) species in solution and in the solid state. Two sets of resonances have been found in **5** and **6** consistent with the presence of inequivalent azolyl rings in a 1:2 ratio, suggesting an exchange between coordinated and uncoordinated azolyl rings, not discernible at room temperature. In the ^{13}C spectrum of **7** a second broad set is often present with dynamically averaged azolyl rings, supporting the existence of both **A** and **B** forms that seem not to exchange at room temperature. In addition, another set of signals, always found in the ^{13}C NMR spectrum of **7**, could be due to 1,2-borotropic rearrangement of the azolyl rings. This hypothesis of the occurrence of 1,2-borotropic rearrangement is supported by the crystallographic identification of compound **8*** and by the fact that in the spectrum of **8** (which contains the less sterically hindered nbd), a set of signals has been detected that could be assigned to **8*** formation.

Solid-State NMR and DFT Calculations. The coordination modes of the ligands in the rhodium complexes were determined by ^{15}N CPMAS experiments (Figure 5). In Table 5 we report experimental and calculated ^{15}N chemical shift values for the ligands Tp^{4Bo}, Tp, Tp*, Tp^{a,3Me}, Tp^{a*,3Me}, and Tp^{4Bo,5Me} and for the corresponding [Rh(cod)Tp^x] complexes **1**, **3**, **5**, **7**, **9**, and **11**. The calculation of ^{15}N NMR chemical shifts has been obtained by geometry optimization at the B3LYP/6-31G* level in the gas phase, followed by NMR (GIAO) calculations at B3LYP/6-31++G** level.

It is well-known that a lower frequency shift is expected when the free nitrogen of the ligand coordinates a metal center. In the case of saturated ligands, the low frequency shift is about 25−40 ppm. However, the shift is approximately 100 ppm for aromatic ligands. This different behavior resembles that observed upon protonation.[34] For

Table 5. Experimental and Calculated ^{15}N NMR Chemical Shifts[a]

		δ ^{15}N calculated, ppm (ppm)		δ ^{15}N experimental, ppm (integral)	
compound	Rh−N1 (Å) calc.	N1	N2	N1	N2
Tl[Tp^{4Bo}]		308.6, 306.4, 306.1	185.8, 185.5, 185.5	306.6 br [b], 296.0 br, 291.9	188.0, 183.4 (2)
Na[Tp]		284.1, 283.7, 283.5	217.9, 217.5, 212.1	278.5, 275.6, 273.9,	213.2 (2), 208.9
K[Tp*]		293.7, 281.7, 281.2	207.0, 201.7, 198.4	278.6, 272.7, 276.8	205.7, 203.4, 199.9
Tl[Tp^{a,3Me}]		279.8, 275.5, 269.5	207.7, 206.9, 214.2	271.4 m (170 Hz) (3)[c]	205.7 (3)
Tl[Tp^{a*,3Me}]		270.3, 261.8, 261.4	220.5, 216.4, 214.8	282.6 br[b], 252.7 br (2),	208.1 (3)
Tl[Tp^{4Bo,5Me}]		308.2, 307.7, 307.4	186.3, 185.5, 184.9	305.4 br, 293.9 br (2)[b]	188.5, 181.4 (2)
[Rh(cod)Tp^{4Bo}] (**1**)	2.366, 2.348, 2.136^{in}	259.1, 259.0, 230.3	176.5, 174.5, 174.3	261.0 (2), 221.9	183.8, 181.1, 175.5
[Rh(nbd)Tp^{4Bo}] (**2**)	2.329, 2.319, 2.111^{in}	255.4, 253.0, 239.4	176.2, 176.2,175.3		
[Rh(cod)Tp^{4Bo,5Me}] (**3**)	2.356, 2.363, 2.136^{in}	259.2, 258.6, 233.8	177.1, 175.0, 174.7	258.3 (2), 224.3	181.2 (3)
[Rh(nbd)Tp^{4Bo,5Me}] (**4**)	2.323, 2.325, 2.110^{in}	256.3, 255.2, 236.1	177.0, 176.2, 175.6		
[Rh(cod)Tp^{a,3Me}] (**5**)	3.748, 2.136^{in}, 2.152^{in}	266.9, 210.9, 204.5	201.9, 200.0, 196.7	277.8, 206.3, 200.8	200.8 (3)
[Rh(nbd)Tp^{a,3Me}] (**6**)	3.723, 2.137^{in}, 2.135^{in}	266.4, 211.2, 204.6	202.2, 197.9, 196.5		
[Rh(cod)Tp^{a*,3Me}] (**7**)	3.790, 2.141^{in}, 2.148^{in}	255.6, 203.7, 194.6	207.5, 205.6, 202.8	267.1, 228.4, 213.3	213.3, 184.9, 180.0
[Rh(nbd)Tp^{a*,3Me}] (**8**)	3.704, 2.132^{in}, 2.126^{in}	261.2, 235.3, 194.2	209.7, 205.9, 179.3		
[Rh(cod)Tp] (**9**)	2.378, 2.351, 2.137^{in}	247.9, 244.8, 222.7	202.1, 201.6, 199.5	245.0 (2), 213.6	203.8 (3)
[Rh(nbd)Tp] (**10**)	2.331, 2.331, 2.115^{in}	242.3, 242.3, 225.0	200.8, 200.1, 200.1		
[Rh(cod)Tp*] (**11**)	3.742, 2.149^{in}, 2.148^{in}	277.7, 220.2, 214.1	198.7, 196.7, 194.0	288.0, 211.7, 211.7	203.6, 200.8, 200.8
[Rh(nbd)Tp*] (**12**)	3.597, 2.134^{in}, 2.139^{in}	281.4, 219.1, 218.1	197.9, 197.6, 197.5		

[a] Calculations were executed at the B3LYP/6-31++G** level (using the geometries optimized at B3LYP/6-31G* in the gas phase), for the free ligands (anion form) and the corresponding Rh derivatives **1**−**12**. N1 and N2 are the nitrogen atoms bonded to Rh and B atoms, respectively. The notation "in" is refers to N1 in-plane atoms coordinated to Rh (see text). [b] Signals are broad probably because of multiple couplings with thallium clusters containing three or more chemically and magnetically inequivalent metal atoms. [c] The signal is a multiplet probably because of couplings with a highly symmetric tetrahedral thallium cluster. A similar behavior has been reported by Claramunt et al. in other thallium scorpionate complexes.[37a]

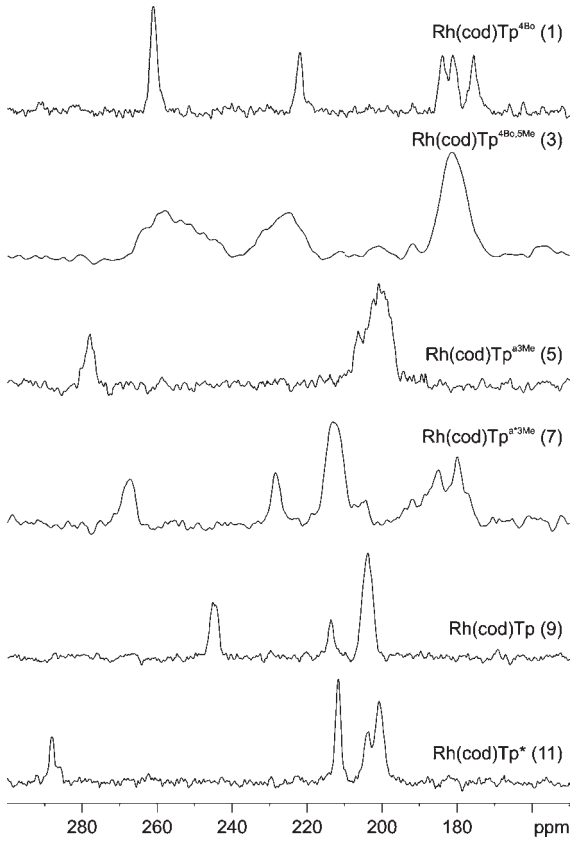

Figure 5. ^{15}N CPMAS spectra of the rhodium complexes **1**, **3**, **5**, **7**, **9**, **11** recorded at 40.56 MHz with a spinning speed of 7 kHz.

aromatic amines, the large coordination shift is associated with the prevalence of the paramagnetic term since the excitation energy for the lone pair of electrons on the nitrogen of the free base is much lower than when this pair binds a metal atom. Earlier studies showed that for tris(pyrazolyl)borate complexes of the type [Rh(diolefin)-Tp^{3R,4R,5R}] the solution ^{15}N NMR chemical shifts can be used to assess the position of the fast equilibria between corresponding four- and five-coordinate forms.[35]

While the chemical shift of the N1 atom (where N1 are the nitrogen atoms directly bonded to the metal) in an alkali metal salt of a hydrotris(pyrazolyl)borate is about 285 ppm, this value changes to 310 ppm for [(η^2-HTp*)Ir-(cod)](CF$_3$SO$_3$) (HTp* = monoprotonated Tp*), a square planar complex of this bidentate nitrogen ligand.[36] Furthermore, the value of this parameter for [Ir(cod)Tp*)], about 235 ppm, corresponds to an average value in solution of one free and two coordinated donor atoms in fast exchange on the NMR time scale.

Because solid-state signals are not averaged by solvent effects or by rapid exchange processes present in solution, the change in the nitrogen chemical shift caused by metal coordination obtained with CPMAS techniques has the great advantage of affording directly information on the ligand hapticity.[37] Calculations of chemical shifts using quantum-chemical methods support the assignments of experimental data, giving new insights in the extraction of structural information. Bond lengths computed by the B3LYP DFT method are overestimated, a typical feature observed in DFT calculations,[38,39] but the overall trend is

(34) Chierotti, M. R.; Gobetto, R. *Chem. Commun.* **2008**, 1621–1634.

(35) Bucher, U. E.; Currao, A.; Nesper, R.; Rüegger, H.; Venanzi, L. M.; Younger, E. *Inorg. Chem.* **1995**, *34*, 66–74, and references quoted therein.

(36) Bovens, M.; Gerfin, T.; Gramlich, V.; Petter, W.; Venanzi, L. M.; Howard, M. T.; Jackson, S. A.; Eisenstein, O. *New J. Chem.* **1992**, *16*, 337–345.

(37) (a) Bertolasi, V.; Boaretto, R.; Chierotti, M. R.; Gobetto, R.; Sostero, S. *Dalton Trans.* **2007**, 5179–5189. (b) Claramunt, R. M.; Sanz, D.; Santa Maria, M. D.; Elguero, J.; Trofimenko, S. *J. Organomet. Chem.* **2004**, *689*, 463–470.

(38) Ma, B.; Lii, J.-H.; Schaefer, H. F., III; Allinger, N. L. *J. Phys. Chem.* **1996**, *100*, 8763–8769.

(39) Garino, C.; Gobetto, R.; Nervi, C.; Salassa, L.; Rosenberg, E.; Ross, J. B. A.; Chu, X.; Hardcastle, K. I.; Sabatini, C. *Inorg. Chem.* **2007**, *46*, 8752–8762.

Chart 3

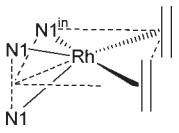

well reproduced. After geometry optimizations using the B3LYP/6-31G** method the calculation of ^{15}N NMR chemical shift affords values in substantial agreement with experimental data.

The resulting low-frequency ^{15}N coordination shifts (related to N1 atoms) for compounds **1**, **3**, **5**, **7**, **9**, and **11**, defined as the differences between the experimental ^{15}N chemical shift of a nitrogen atom within the complex and the corresponding pure ligand, are discussed in relation to the molecular structure. Where more than one signal is present an average value has been considered.

In the pure ligands, the signals of the nitrogen atoms bonded to the boron atom (hereafter N2) fall around 200 ppm, while the other nitrogen atoms (N1) give rise to resonances around 280 ppm. Since N2 atoms connected to boron are less affected by the metal coordination, the discussion will be mainly focused on the N1 chemical shift.

For **1** the crystal structure is not available, but geometry optimization, followed by ^{15}N chemical shift calculation shows a good agreement with the experimental data (δ 261.0, integral value 2 and δ 221.9, integral value 1). The experimental ^{15}N CPMAS spectrum clearly reveals the κ^3 hapticity of the Tp^{4Bo} ligand to the Rh metal. The analysis of the ^{15}N CPMAS spectra of **1** cf. Tp^{4Bo} is in agreement with a five-coordinate metal atom, with three nitrogen atoms and the two diene bonds connected to Rh. The structure can be viewed as square planar in which one of the coordination positions is occupied by a pair of nitrogen atoms lying above and below the coordination plane as depicted in Chart 3.

The nitrogen atom formally lying in the coordination plane, marked as N1^{in} in Table 5, has a shorter computed Rh−N1^{in} bond length (2.136 Å) than the other two (2.366 and 2.348 Å). These two out-plane N1 atoms display a coordination shift of about 30 ppm, whereas the in-plane N1^{in} nitrogen shows a low-frequency coordination shift of about 85 ppm.

The experimental ^{15}N CPMAS data of complexes **3** and **9** are consistent with five-coordinate Rh atoms (i.e., the κ^3 hapticity of Tp^x ligands) found by single crystal X-ray for **3**. For these complexes the coordination shifts of the two out-of-the-plane nitrogen atoms are 39 and 31 ppm, respectively, whereas those of the in-plane N1^{in} nitrogens are 73 and 62 ppm, respectively. For **3** and **9**, again, the shorter Rh−N1^{in} distances (2.136 and 2.137 Å, respectively) are associated with the greater low-frequency coordination shifts.

The same approach can be extended to complexes **5**, **7**, and **11**. In these cases a κ^2 ligand hapticity has been demonstrated by experimental and calculated data. The computed structures display a square planar geometry. Two N1 atoms lie in the coordination plane (N1^{in}) while the third is directed away from the metal.

The SS NMR data for complex **5** show two signals for the N1^{in} atoms at 200.8 (overlapped with the three N2 nitrogens) and 206.3 ppm with calculated Rh−N1^{in} distances of 2.152 and 2.136 Å. The uncoordinated N1 gives rise to a signal with its chemical shift almost unchanged (δ = 277.8, Rh−N1 distance 3.748 Å) with respect to that of the pure ligand.

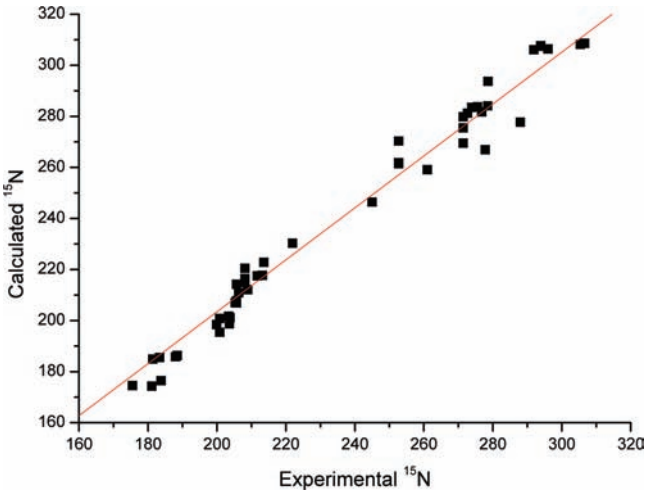

Figure 6. Calculated versus experimental ^{15}N chemical shift values (ppm).

The ^{15}N CPMAS spectrum of complex **11** displays a peak at 211.7 ppm, with double intensity, for the metal bonded N1^{in} whereas the chemical shift of the uncoordinated N1, 288.0 ppm (integral value 1), remains substantially unchanged, in agreement with a calculated Rh−N1 distance of 3.742 Å, too long to be considered a bonding distance. The coordination shifts of the N1^{in} atoms are 64 and 50 ppm for complexes **5** and **11**, respectively. A similar trend has been found for complex **7**, confirming also in this case a κ^2 ligand hapticity.

The general trend of the computed ^{15}N chemical shifts parallels that of the experimental data, as shown by the plot of calculated versus experimental ^{15}N chemical shifts (Figure 6, correlation factor r = 0.990, slope = 1.0171). It is clear that there are two kinds of nitrogen atoms bonded to Rh, and those that have shorter bond distances show the larger low-frequency coordination shifts. Small discrepancies (beyond the compromise of choosing the basis set) are probably because the actual geometries in the solid are slightly different from the calculated ones because of the neglect of solid-state interactions. This is especially true for the free ligands, where intermolecular and cation interactions could affect the computed NMR chemical shift.

We finally note that all the calculated ^{15}N chemical shifts of the nbd complexes for which experimental data are not available (i.e., complexes **2**, **4**, **6**, **8**, **10**, and **12**) parallel those of the corresponding cod complexes. In fact, DFT calculations predict a κ^3 coordination mode for **2**, **4**, and **10**, and a κ^2 coordination mode for **6**, **8**, and **12**, in a similar fashion as observed for the cod complexes.

Conclusions

The coordination modes of poly(pyrazolyl)borate ligands about transition metal atoms have been investigated in recent years, and a plethora of mononuclear and polynuclear structure types have been elucidated. Structural changes in the coordination mode are of paramount importance for tuning

the correct catalytic metal site or for varying the physicochemical properties of the metal complexes. Since this field has greatly expanded and single crystal X-ray determinations are not always available for resolving the structural chemistry, there is a need for alternative spectroscopic methods able to determine the ligand coordination mode. In this paper we have demonstrated that ^{15}N CPMAS data together with ^{15}N chemical shift values obtained by DFT calculation can afford information concerning the hapticity of poly(pyrazolyl)-borate ligands bound to the Rh metal.

Coordination of three nitrogen atoms to the rhodium has been found for [Rh(cod)Tp], **9**, with one of the nitrogen atoms having a low-frequency coordination shift of about 65 ppm in agreement with a shorter Rh−N distance. The same κ^3 hapticity has been found for Tp^{4Bo}, **1**, and $Tp^{4Bo,5Me}$, **3**, showing coordination shifts of about 80−85 ppm associated with the shorter Rh−N distances (2.136 Å). Experimental NMR data and calculated data for complexes **5**, **7**, and **11** are in good agreement with the coordination of only two nitrogen atoms of the ligand to the metal, whereas the chemical shift of the third nitrogen remains substantially unchanged in agreement with a calculated M−N distance too long to be considered a bonding distance. On the basis of the substantial agreement of the computed ^{15}N chemical shifts using quantum-chemical methods with the experimental data, we believe that the procedure and the results reported in this contribution will afford new insights in the extraction of structural information of the ligand hapticity in complexes where X-ray structures are not available.

Supporting Information Available: Further details are given in Figures S1 and S2, and crystallographic data is given in CIF format. This material is available free of charge via the Internet at http://pubs.acs.org.